

Structure and properties of ionic fullerene complex $\text{Co}^+(\text{dppe})_2 \cdot (\text{C}_{60}^{\cdot-}) \cdot (\text{C}_6\text{H}_4\text{Cl}_2)_2$: distortion of the ordered fullerene cage of $\text{C}_{60}^{\cdot-}$ radical anions†

Dmitri V. Konarev,^{*a} Alexey V. Kuźmin,^b Sergey V. Simonov,^b Salavat S. Khasanov,^b Evgeniya I. Yudanov^a and Rimma N. Lyubovskaya^a

Received 10th January 2011, Accepted 16th February 2011

DOI: 10.1039/c1dt10039d

New ionic complex $\{\text{Co}^+(\text{dppe})_2\} \cdot (\text{C}_{60}^{\cdot-}) \cdot (\text{C}_6\text{H}_4\text{Cl}_2)_2$ (**1**) was obtained by the reduction of a $\text{Co}(\text{dppe})\text{Br}_2$ and C_{60} mixture by TDAE in *o*-dichlorobenzene followed by precipitation of crystals by hexane. Optical and EPR spectra of **1** indicated the formation of $\text{C}_{60}^{\cdot-}$ radical anions and diamagnetic $\text{Co}^+(\text{dppe})_2$ cations. The structure of **1** solved at 100(2) K involves chains of $\text{C}_{60}^{\cdot-}$ arranged along the lattice *a*-axis with a center-to-center distance of 10.271 Å. The chains are separated by bulky $\text{Co}^+(\text{dppe})_2$ cations and solvent molecules. All components of **1** are well ordered allowing the distortion of the $\text{C}_{60}^{\cdot-}$ radical anion to be analyzed. An elongation of the $\text{C}_{60}^{\cdot-}$ sphere by 0.0254(2) was found. It is essentially smaller than those in the salts $(\text{Cp}^*\text{Ni}^+) \cdot (\text{C}_{60}^{\cdot-}) \cdot \text{CS}_2$ and $(\text{PPN}^+)_2 \cdot (\text{C}_{60}^{2-})$ with greater distortion of the fullerene cage. The calculation of the electronic structure of fullerene by the extended Hückel method showed slight splitting of the C_{60} LUMO, due to the distortion, by three levels. Two levels are located 180 and 710 cm^{-1} higher than the ground level. The averaged 6–6 and 5–6 bonds in $\text{C}_{60}^{\cdot-}$ with lengths of 1.397(2) and 1.449(2) Å are close to those determined for the C_{60}^{2-} dianions in $(\text{PPN}^+)_2 \cdot (\text{C}_{60}^{2-})$, but are slightly longer and shorter, respectively, than the length of these bonds in neutral C_{60} .

Introduction

Ionic fullerene C_{60} complexes show a variety of promising physical properties such as metallic conductivity, superconductivity and ferromagnetism.^{1–4} Great interest is directed to the intrinsic structural and electronic properties of discrete fullerene $\text{C}_{60}^{\text{n-}}$ anions.^{5,6} The Jahn–Teller theorem predicts distortion of the C_{60} cage from icosahedral symmetry when additional electrons are added to the t_{1u} LUMO orbital of C_{60} to remove its degeneracy. The presence or absence of such distortion in the fullerene anions are of particular interest since degeneracy strongly affects the electronic structure of fullerene and to a great extent defines such phenomena as superconductivity and ferromagnetism.

Fullerene C_{60} is nearly a spherical molecule and fullerene anions are disordered in most ionic complexes and salts. Precise geometry of ordered fullerene anions was determined in a few compounds only.^{7–11} These are mainly compounds containing C_{60}^{2-} dianions. The first crystal structure of the $(\text{PPN}^+)_2 \cdot (\text{C}_{60}^{2-})$

salt with a triclinic unit cell, showed a strong enough deviation from the fullerene cage I_h symmetry (the difference between the longest and the shortest diameter of C_{60} was 0.086 Å) allowing the authors to conclude on the presence of an intrinsic Jahn–Teller effect in the C_{60}^{2-} dianions.⁷ Smaller but noticeable distortions of the fullerene cage (from 0.060 to 0.075 Å) were observed in the $[\text{M}(\text{NH}_3)_6^{2+}] \cdot (\text{C}_{60}^{2-}) \cdot (\text{NH}_3)_3$ salts ($\text{M} = \text{Ni}, \text{Mn}, \text{and Cd}$) with triclinic lattice^{8,9} and in the $(\text{Cp}^*\text{Co}^+)_2 \cdot (\text{C}_{60}^{2-}) \cdot (\text{C}_6\text{H}_4\text{Cl}_2, \text{C}_6\text{H}_5\text{CN})_2$ complex with monoclinic lattice.¹⁰ However, the study of the crystal structure of $\{(\text{Ba}^{2+}) \cdot (\text{NH}_3)_7\} \cdot (\text{C}_{60}^{2-}) \cdot \text{NH}_3$ with higher trigonal lattice symmetry showed that the cage of the C_{60}^{2-} dianion is essentially less distorted (0.014 Å).¹¹ Based on this observation it was concluded that strong or moderate distortion of the C_{60}^{2-} cage observed in previously studied compounds may be a result of a low-symmetry, triclinic environment of C_{60}^{2-} rather than the intrinsic Jahn–Teller effect.¹¹ Indeed, the distortion of 0.014 Å¹¹ is even smaller than that of the neutral fullerene cage in C_{60} (0.025 Å)¹² which is not subject to the Jahn–Teller effect.

The strongest distortion of the fullerene cage from I_h symmetry was found for well-ordered $\text{C}_{60}^{\cdot-}$ radical anions in the $(\text{Cp}^*\text{Ni}^+) \cdot (\text{C}_{60}^{\cdot-}) \cdot \text{CS}_2$ complex with monoclinic lattice (0.098 Å).¹³ In this compound a pentamethylcyclopentadienyl ring of Cp^*Ni^+ is located exactly over the $\text{C}_{60}^{\cdot-}$ pentagon and multiple short van der Waals C...C contacts are formed between them. Therefore, strong π – π interactions of $\text{C}_{60}^{\cdot-}$ with closely located Cp^*Ni^+ cations can additionally contribute to the ellipsoidal distortion

^aInstitute of Problems of Chemical Physics RAS, Chernogolovka, Moscow region, 142432, Russia. E-mail: konarev@icp.ac.ru; Fax: +7-49652-21852

^bInstitute of Solid State Physics RAS, Chernogolovka, Moscow region, 142432, Russia

† Electronic supplementary information (ESI) available: IR, UV-Vis-NIR and EPR spectra of complex **1** and starting compounds. CCDC reference number 805414. For ESI and crystallographic data in CIF or other electronic format see DOI: 10.1039/c1dt10039d

of $C_{60}^{\cdot-}$. Both antiferromagnetic and ferromagnetic phases of $(TDAE^+)(C_{60}^{\cdot-})$ have a monoclinic lattice and contain ordered $C_{60}^{\cdot-}$ radical anions which show a smaller distortion of the $C_{60}^{\cdot-}$ cage (0.02–0.04 Å).^{14,15}

In this work we obtained the new ionic complex of fullerene, $\{Co^+(dppe)_2\}(C_{60}^{\cdot-})(C_6H_4Cl_2)_2$ where dppe is bis(diphenylphosphino)ethane (**1**), as single crystals. The analysis of the EPR-, IR- and optical spectra of **1** showed the formation of the $C_{60}^{\cdot-}$ radical anions and the diamagnetic $Co^+(dppe)_2$ cations. The structure of **1** determined at 100(2) K contains completely ordered $C_{60}^{\cdot-}$ radical anions for which the distortion from I_h symmetry is discussed.

Results and discussion

a. Synthesis

Tetrakis(dimethylamino)ethylene (TDAE) reduces C_{60} in *o*-dichlorobenzene ($C_6H_4Cl_2$) to the radical anion state. However, the diffusion of hexane into $C_6H_4Cl_2$ solution containing $TDAE^{2+}$ and $C_{60}^{\cdot-}$ ions does not afford the crystals of the ionic complex. On the contrary, in these conditions fullerene C_{70} forms two phases: $(TDAE^{2+})(C_{70}^{\cdot-})(C_6H_4Cl_2)(C_6H_{14})_{0.5}$ and $(TDAE^{2+})(C_{70}^{\cdot-})(C_6H_4Cl_2)$.¹⁶ When the mixture of $Co(dppe)Br_2$ and C_{60} is reduced by an excess of TDAE, all components dissolve to produce a violet-red solution from which well-shaped black elongated parallelepipeds of $\{Co^+(dppe)_2\}(C_{60}^{\cdot-})(C_6H_4Cl_2)_2$ (**1**) are crystallized by diffusion of hexane. TDAE reduces both C_{60} to $C_{60}^{\cdot-}$ and Co^{2+} to Co^+ . Previously it was shown that Co^{2+} in $\{Co(dppe)_2(CH_3CN)\}$ can be reduced electrochemically to Co^+ at -0.7 V.¹⁷ This is possible for TDAE as well since it has a more negative first oxidation potential ($E^{+/0} = -0.75$ V).¹⁸ Further reduction of Co^+ to Co^0 realized at -1.56 V¹⁷ cannot occur in these conditions.

$Ni(dpmp)Cl_2$ (dpmp is bis(diphenylphosphino)propane) and C_{60} after reduction by sodium fluorenone forms a $Ni(dpmp)(\eta^2-C_{60})$ complex where zero valent nickel coordinates to C_{60} by the η^2 -type. In these coordination units, the $Ni-C(C_{60})$ bonds of 1.950(2) Å length are essentially shorter than the $Ni-P$ bonds (2.152(2) and 2.155(2) Å).¹⁹ It is interesting that the $Co(dppe)^+$ unit does not add to $C_{60}^{\cdot-}$ to form a coordinated $Co(dppe)(\eta^2-C_{60})$ complex. Instead of that, the $Co^+(dppe)_2$ cations are formed in solution and co-crystallize with non-bonded $C_{60}^{\cdot-}$.

b. Charged state of C_{60} and diamagnetism of $Co^+(dppe)_2$

The spectra of **1** in the IR- and UV-visible-NIR ranges are shown in supporting information.† IR active modes of C_{60} manifest absorption bands at 533 (coincides with the band of $Co^+(dppe)_2$), 576, 1180, and 1390 cm^{-1} . The $F_{1g}(4)$ mode which is most sensitive to the charged state of C_{60} is shifted from 1429 cm^{-1} in the neutral state to 1396–1388 cm^{-1} in the radical anion state.^{20–22} The position of this mode in the spectrum of **1** at 1390 cm^{-1} indicates the formation of the $C_{60}^{\cdot-}$ radical anions. The spectrum of **1** with two bands in the NIR range at 930 and 1090 nm is also characteristic of $C_{60}^{\cdot-}$.^{4,5}

The EPR spectrum provides further evidence of the ionic ground state of **1**. The compound manifests a broad intense EPR signal with a g -factor of 1.9986 and a linewidth (ΔH) of 4.57 mT at

room temperature (supporting information†). Such signals are generally observed in the complexes and salts containing $C_{60}^{\cdot-}$ radical anions.^{4,5} Integral intensity of this signal corresponds to the contribution of about one $S = 1/2$ spin per formula unit. In the background of the broad signal from $C_{60}^{\cdot-}$, a very weak narrow signal with approximate g -factor of about 2.0000 can also be resolved. This signal originates from about 0.3% of spins of total amount of C_{60} and can be attributed to defects.

Starting compound $Co(dppe)Br_2$, with paramagnetic Co^{2+} ions, manifests a broad intense EPR signal with g -factor = 2.0357 and $\Delta H = 15.5$ mT. It is expected that cobalt ions in 3+ and 1+ charged states with d^6 and d^8 electronic configurations, respectively, should be diamagnetic and EPR silent. Indeed, the EPR spectrum of **1** shows no additional signals to that from $C_{60}^{\cdot-}$. Thus, the EPR data justify the reduction of paramagnetic and EPR active Co^{2+} to the EPR silent Co^+ . Electroneutrality of the complex also justifies the formation of monocationic $Co^+(dppe)_2$ species since the complex involves cations and fullerene anions at a 1 : 1 ratio and the charged state of C_{60} was estimated to be 1–.

c. Crystal structure of the complex

The crystal structure of **1** was studied at 100(2) K. It has a monoclinic unit cell with well-ordered $Co(dppe)_2^+$ and $C_{60}^{\cdot-}$ ions and solvent $C_6H_4Cl_2$ molecules (R -factor is 3.28%). The $Co^+(dppe)_2$ cation with the 1+ charged four-coordinated cobalt atom was generated in solution electrochemically at -0.7 V starting from $\{Co(dppe)_2(CH_3CN)\}^{2+}$ which loses CH_3CN molecules during the reduction.¹⁷ The structure of individual $Co(dppe)_2^+$ cations was unknown. However, some $L_2Co^+(dppe)_2$ cations with six-coordinated cobalt atoms were structurally characterized: $\{H_2Co^+(dppe)_2\}$, $\{HCo^+(dppe)_2(CH_3CN)\}$ and $\{O_2Co^+(dppe)_2\}$.^{17,23}

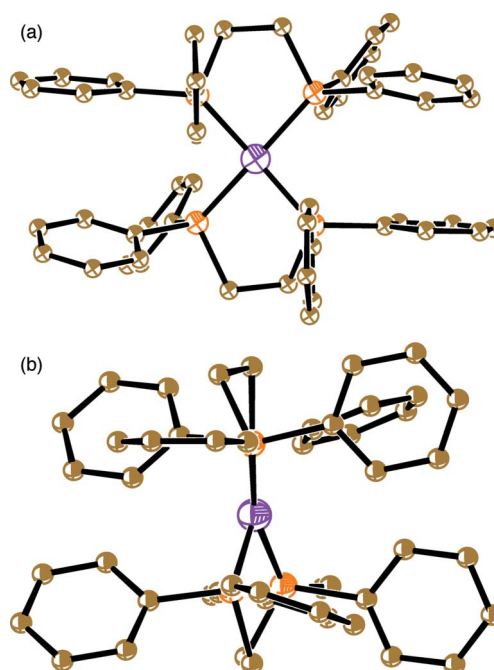


Fig. 1 The structure of $Co^+(dppe)_2$ cation viewed on upper (a) and along (b) one PCoP plane.

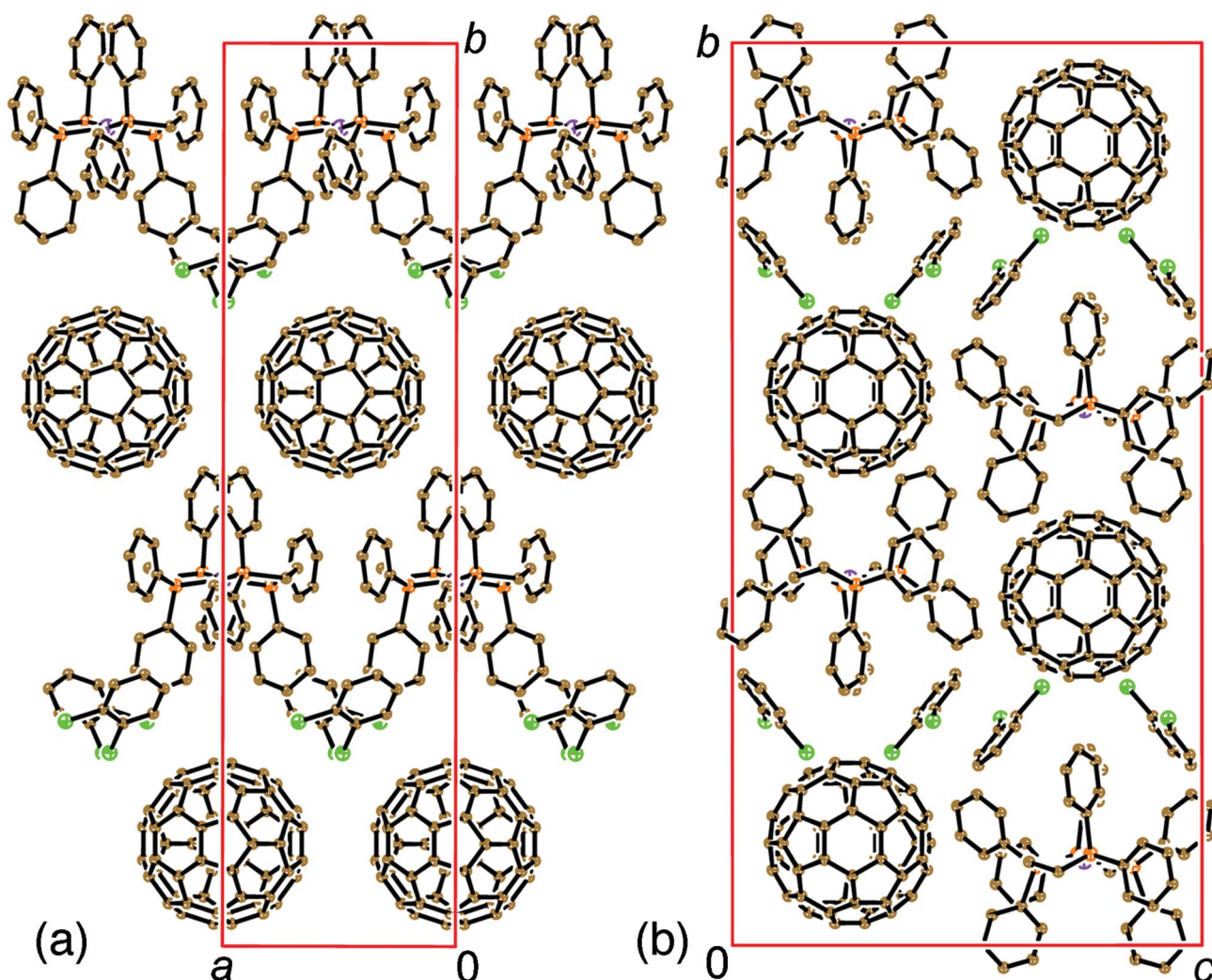


Fig. 2 The crystal structure of **1** viewed along the lattice *c*- (a) and *b*-axes (b).

Since the cobalt atom has d^8 configuration in $\text{Co}^+(\text{dppe})_2$, square-planar geometry for this ion is expected. Nevertheless, the P_4Co fragment is not planar (Fig. 1). The angle between two P_2Co planes is $21.82(2)^\circ$. Such geometry is different from the tetrahedral geometry of neutral $\text{Co}^0(\text{dppp})_2$ and anionic $\text{Co}^-(\text{dppe})_2$.^{24,25} The Co–P bond length in $\text{Co}^+(\text{dppe})_2$ is in the 2.182–2.204(2) Å range. The ability of Co^{II} porphyrins to form coordination Co–C bonds with C_{60}^- is known.^{26–29} In the case of $\text{Co}^+(\text{dppe})_2$, such coordination is not possible since a close approach of bulky C_{60}^- to Co^+ is sterically blocked. Moreover, the shortest distances between Co^+ and a carbon atom of C_{60}^- exceeds 8 Å showing a minimal effect of the cations on the geometry of C_{60}^- .

The C_{60}^- radical anions form chains arranged along the lattice *a*-axis (Fig. 2a shows fragments of the two chains). The center-to-center distance of 10.271 Å between the fullerenes in the chain is longer than the van der Waals diameter of C_{60} (10.18 Å) and no van der Waals C...C contacts are formed between them. Fullerene chains are separated by bulky $\text{Co}^+(\text{dppe})_2$ cations and solvent $\text{C}_6\text{H}_4\text{Cl}_2$ molecules. As a result, the shortest center-to-center distance between fullerenes from different chains is quite long (13.6 Å). Each C_{60}^- is surrounded by the phenyl groups of six $\text{Co}^+(\text{dppe})_2$ cations and forms van der Waals contacts

with two $\text{C}_6\text{H}_4\text{Cl}_2$ molecules. Multiple shortened van der Waals $\text{H}(\text{Co}^+(\text{dppe})_2, \text{C}_6\text{H}_4\text{Cl}_2) \dots \text{C}(\text{C}_{60}^-)$ contacts in the 2.84–2.89 Å range and several $\text{C}(\text{phenyl group of } \text{Co}^+(\text{dppe})_2) \dots \text{C}(\text{C}_{60}^-)$ contacts of 3.20 Å length provide complete ordering of C_{60}^- in this complex.

d. Analysis of the fullerene distortion in **1**

Ordering of C_{60}^- provides an opportunity to study the distortion of the C_{60}^- radical anions in **1**. Labels of the carbon atoms in C_{60}^- are shown in Fig. 3a and the distances of the carbon atoms from the center of fullerene are presented in Fig. 3b. These distances vary in a narrow range from 3.537(2) to 3.555(2) Å with the mean value of 3.545(2) Å. All twelve carbon atoms (C301, C302, C306, C307, C311, C312 and their symmetrically located equivalents shown by red circles in Fig. 3a) which have the longest distance from the center belong to two oppositely located hexagons. This indicates the elongation of the C_{60}^- sphere along the axis passed through the centers of two 6–6 bonds (these bonds involved C311 and C312 atoms and their symmetrically located equivalents). This axis forms an angle of 41.5° with the lattice *a*-axis along which linear C_{60}^- chains are formed (Fig. 2a). The distances

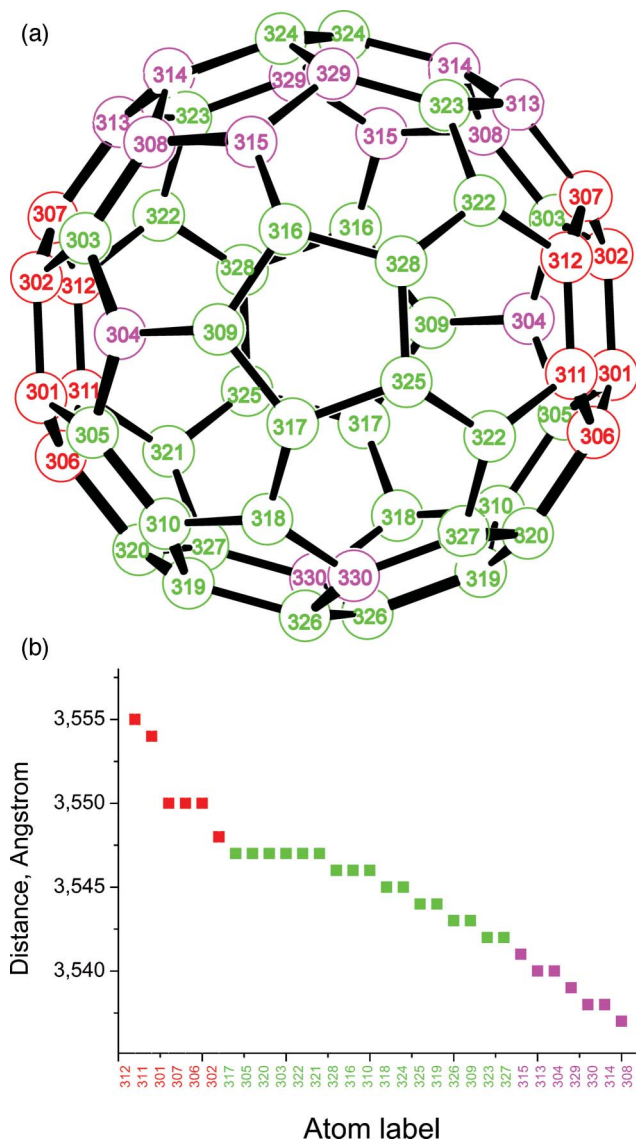


Fig. 3 Atom labeling in the $C_{60}^{\cdot-}$ radical anion. (a) Red labels mark atoms with the longest distances from the center, violet labels mark atoms with the shortest distances from the center and green labels mark atoms with mean distances from the center. (b) Distances of the carbon atoms of $C_{60}^{\cdot-}$ from the center.

between the midpoints of two oppositely located 6–6 bonds in three orthogonal directions are 6.944, 6.948 and 6.970 Å. The latter distance was measured for the midpoints of two oppositely located 6–6 bonds having maximal distance from the center of the fullerene (Fig. 3b). The difference between the longest and the shortest diameter of C_{60} is only 0.026 Å. The ellipsoid of $C_{60}^{\cdot-}$ was calculated by the least-squares method in an orthogonal system using the following equation: $(X_{\text{new}}/3.5522)^2 + (Y_{\text{new}}/3.5395)^2 + (Z_{\text{new}}/3.5420)^2 = 1$. The greatest radius was obtained to be 3.5520(1) Å and two other radii were 3.5420(1) and 3.5395(1) Å. The difference between the longest and shortest diameter of the $C_{60}^{\cdot-}$ ellipsoid is also 0.0254(2) Å, *i.e.* essentially smaller than those in the $(Cp^*_2Ni^+)(C_{60}^{\cdot-})CS_2$ and $(PPN^+)_2(C_{60}^{2-})$ salts with strong distortion of the fullerene cage (0.086–0.098 Å). The distortion of fullerene in neutral C_{60} is 0.025 Å only.¹² Since there is no Jahn–

Teller effect in neutral C_{60} , it can be concluded that the effect observed in $C_{60}^{\cdot-}$ is rather small.

The electronic structure of fullerene in **1** was calculated using the extended Hückel method based on the crystal structure.³⁰ This method provides reasonable values for the energy levels of molecular orbitals in C_{60} since the calculated HOMO–LUMO gap of 1.50 eV is close to the experimentally³¹ and theoretically³² determined HOMO–LUMO gap in C_{60} . It is known that the LUMO of C_{60} with ideal I_h symmetry consists of three degenerated molecular orbitals (labeled as 121, 122 and 123). The distortion of $C_{60}^{\cdot-}$ results in a small splitting of the LUMO. The 121 molecular orbital is lowest in energy and is occupied by one electron. It is distributed over the belt coming through two oppositely located hexagons with the maximal distance in the fullerene cage as shown in Fig. 4. The 122 molecular orbital is located 180 cm^{-1} (260 K) higher and should be almost empty at 100(2) K. It is also distributed over the belt coming through two oppositely located hexagons with the maximal distance (Fig. 4). It should be noted that the splitting of 180 cm^{-1} is noticeably smaller than the experimentally determined gap of 730 cm^{-1} between singlet and triplet states for the C_{60}^{2-} dianions in $(Cp^*_2Co^+)_2(C_{60}^{2-}) \cdot (C_6H_4Cl_2, C_6H_5CN)_2$.¹⁰ However, the distortion of the C_{60}^{2-} dianions in this complex is also noticeably stronger (the difference between the longest and the shortest diameter of C_{60} was 0.060 Å¹⁰ vs. 0.026 Å in **1**). The highest in energy, the empty 123 orbital, is located above the 121 level by 710 cm^{-1} (1020 K) and is distributed over the belt located perpendicular to the long axis of the fullerene ellipsoid (Fig. 4).

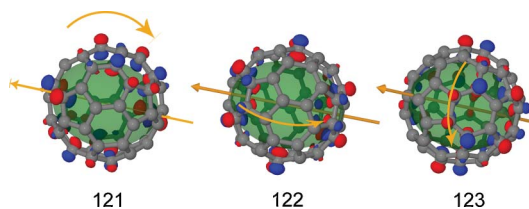


Fig. 4 The direction of the long axis of the fullerene ellipsoid (yellow arrow) and the distribution of the 121, 122 and highest in energy 123 molecular orbitals over the $C_{60}^{\cdot-}$ cage calculated by the extended Hückel method.

The 6–6 and 5–6 bond lengths in $C_{60}^{\cdot-}$ are within the 1.393(2)–1.401(2) and 1.446(2)–1.456(2) Å range and are averaged at 1.397(2) and 1.449(2) Å, respectively. The C_{60}^{2-} dianions with maximally distorted fullerene cage have close averaged lengths of the 6–6 and 6–5 bonds of 1.399(2) and 1.446(2) Å in $(PPN^+)_2(C_{60}^{2-})$.⁷ Neutral C_{60} has slightly shorter 6–6 bonds of 1.391(8) Å and longer 5–6 bonds of 1.455(8) Å.³³ The direction of the bond length change at C_{60} charging is in accordance with the theory which predicts that the t_{1u} LUMO orbital is antibonding for the 6–6 bonds and bonding for the 6–5 bonds.³⁴

Conclusion

A new ionic fullerene complex $\{Co^+(dppe)_2\} \cdot (C_{60}^{\cdot-}) \cdot (C_6H_4Cl_2)_2$ (**1**) was obtained. Optical and EPR spectra indicate the formation of $C_{60}^{\cdot-}$ radical anions and diamagnetic Co^+ ($dppe$)₂ cations whose molecular structures were analyzed. The $C_{60}^{\cdot-}$ cage elongates by 0.0254(2) Å. This distortion is essentially smaller than that in

the $(\text{Cp}^*_2\text{Ni}^+)(\text{C}_{60}^{2-})\cdot\text{CS}_2$ and $(\text{PPN}^+)_2(\text{C}_{60}^{2-})$ salts and is close to that in neutral C_{60} . The calculation of the electronic structure of fullerene by the extended Hückel method showed slight splitting of the C_{60} LUMO due to the distortion by 180 and 710 cm^{-1} . The splitting between occupied 121 and nearly empty 122 orbitals is smaller than the experimentally determined singlet–triplet energy gap for the C_{60}^{2-} dianions in $(\text{Cp}^*_2\text{Co}^+)_2(\text{C}_{60}^{2-})\cdot(\text{C}_6\text{H}_4\text{Cl}_2, \text{C}_6\text{H}_5\text{CN})_2$.¹⁰ The averaged 6–6 and 5–6 bond lengths of 1.397(2) and 1.449(2) Å in C_{60}^{2-} are close to those determined for the C_{60}^{2-} dianions in $(\text{PPN}^+)_2(\text{C}_{60}^{2-})$ but slightly longer and shorter, respectively, than the length of these bonds in neutral C_{60} .

Experimental

Materials

CoBr_2 , bis(diphenylphosphino)ethane (dppe) and TDAE were purchased from Aldrich. C_{60} of 99.9% purity was used from MTR Ltd. Solvents were purified in argon atmosphere. *o*-Dichlorobenzene ($\text{C}_6\text{H}_4\text{Cl}_2$) was distilled over CaH_2 under reduced pressure and hexane was distilled over Na/benzophenone. The solvents were degassed and stored in a glove box. All manipulations for the synthesis of **1** were carried out in a MBraun 150B-G glove box with controlled atmosphere and the content of H_2O and O_2 was less than 1 ppm. The crystals were stored in a glove box and put in anaerobic conditions in 5 mm quartz tubes for EPR measurements under argon. KBr pellets for IR and UV-Vis-NIR measurements were prepared in a glove box.

Synthesis

For the preparation of $\text{Co}(\text{dppe})\text{Br}_2$, anhydrous CoBr_2 (300 mg, 1.38 mmol) was dissolved in 10 ml of acetonitrile (AN) and an equimolar amount of dppe was added (547 mg, 1.38 mmol) to this solution. After 1 h the green crystalline precipitate was filtered, washed with 5 ml of cold AN and dried in air. Yield was 720 mg (82%).

The crystals of **1** were obtained by diffusion. C_{60} (30 mg, 0.035 mmol), $\text{Co}(\text{dppe})\text{Br}_2$ (43 mg, 0.07 mmol) and an excess of TDAE (0.5 ml) were dissolved in 14 ml of DCB upon stirring at $60\text{ }^\circ\text{C}$ for a night to produce violet-red solution. The solution was cooled down to room temperature, filtered in a 50 ml glass tube of 1.8 cm diameter with a ground glass plug, and 30 ml of hexane was layered over the solution. Diffusion was carried out for 1 month to yield the crystals of **1** on the wall of the tube. The solvent was decanted from the crystals, which were washed with hexane to give black well-shaped elongated parallelepipeds of **1** up to $0.3 \times 0.3 \times 1\text{ mm}^3$ in size with 50% yield. The composition of the complex was determined from the X-ray diffraction on a single crystal of $\text{Co}(\text{dppe})_2\cdot\text{C}_{60}\cdot(\text{C}_6\text{H}_4\text{Cl}_2)_2$ (**1**). Several single crystals selected from the synthesis had similar unit cell parameters.

General

FT-IR spectra were measured in KBr pellets with a Perkin–Elmer 1000 series spectrometer ($400\text{--}7800\text{ cm}^{-1}$). The UV-visible spectrum was measured in KBr pellet on a Shimadzu-3100 spectrometer in the $600\text{--}1500\text{ nm}$ range. The EPR spectrum of **1** was recorded at room temperature with a Radiopan SE/X-2547 spectrometer. For the estimation of a number of spins in **1**, integral

intensity of the signal from a weighed amount of the complex was compared with that of the signal from a sample of α,α' -diphenyl- β -picrylhydrazid (DPPH) with a known number of spins.

X-Ray crystal structure determination

Crystal data for **1**. $\text{C}_{124}\text{H}_{56}\text{Cl}_4\text{CoP}_4$, $M_r = 1870.30\text{ g mol}^{-1}$, black parallelepiped, monoclinic, $C2/c$, $a = 10.2711(5)$, $b = 39.2279(18)$, $c = 20.6979(11)\text{ \AA}$, $\beta = 100.241(5)^\circ$, $V = 8206.6(7)\text{ \AA}^3$, $Z = 4$, $d_c = 1.514\text{ g cm}^{-3}$, $\mu = 0.479\text{ mm}^{-1}$, $F(000) = 3820$, $T = 100(2)\text{ K}$, $2\theta_{\text{max}} = 54.2^\circ$, reflections measured 31494, unique reflections 8950, reflections with $I > 2\sigma(I) = 7369$, parameters refined 600, restraints 0, $R_1 = 0.0328$, $wR_2 = 0.0877$, GOF = 1.065.

X-Ray diffraction data for **1** were collected on an Oxford diffraction “Gemini-R” CCD diffractometer with graphite monochromated Mo-K α radiation using an Oxford Instrument Cryojet system. Raw data reduction to F^2 was carried out using CrysAlisPro, Oxford Diffraction Ltd. The structure was solved by direct method and refined by the full-matrix least-squares method against F^2 using SHELX-97.³⁵ Non-hydrogen atoms were refined in the anisotropic approximation. Positions of hydrogen atoms were calculated geometrically. Subsequently, the positions of H atoms were refined by the “riding” model with $U_{\text{iso}} = 1.2U_{\text{eq}}$ of the connected non-hydrogen atom or as ideal CH_3 groups with $U_{\text{iso}} = 1.5U_{\text{eq}}$.

Acknowledgements

The work was supported by the RFBR grant No 09-02-01514.

Notes and references

- 1 M. J. Rosseinsky, *J. Mater. Chem.*, 1995, **5**, 1497.
- 2 B. Gotschy, *Fullerene Sci. and Technol.*, 1996, **4**, 677.
- 3 D. V. Konarev, S. S. Khasanov, A. Otsuka, M. Maesato, G. Saito and R. N. Lyubovskaya, *Angew. Chem. Int. Ed.*, 2010, **49**, 4829.
- 4 D. V. Konarev and R. N. Lyubovskaya, *Russ. Chem. Rev.*, 1999, **68**, 19.
- 5 C. A. Reed and R. D. Bolskar, *Chem. Rev.*, 2000, **100**, 1075.
- 6 D. V. Konarev, S. S. Khasanov and R. N. Lyubovskaya, *Russ. Chem. Bull.*, 2007, **56**, 371.
- 7 P. Paul, Z. Xie, R. Bau, P. D. W. Boyd and C. A. Reed, *J. Am. Chem. Soc.*, 1994, **116**, 4145.
- 8 K. Himmel and M. Jansen, *Eur. J. Inorg. Chem.*, 1998, 1183.
- 9 K. Himmel and M. Jansen, *Chem. Commun.*, 1998, 1205.
- 10 D. V. Konarev, S. S. Khasanov, G. Saito, I. I. Vorontsov, A. Otsuka, R. N. Lyubovskaya and Yu. M. Antipin, *Inorg. Chem.*, 2003, **42**, 3706.
- 11 K. Himmel and M. Jansen, *Inorg. Chem.*, 1998, **37**, 3437.
- 12 H.-B. Bürgi, E. Blanc, D. Schwarzenbach, S. Liu, Y.-J. Lu, M. M. Kappers and J. A. Ibers, *Angew. Chem., Int. Ed. Engl.*, 1992, **31**, 640.
- 13 W. C. Wan, X. Liu, G. M. Sweeney and W. E. Broderick, *J. Am. Chem. Soc.*, 1995, **117**, 9580.
- 14 B. Narimbetov, H. Kobayashi, M. Tokumoto, A. Omerzu and D. Mihailovic, *Chem. Commun.*, 1999, 1511.
- 15 M. Fujiwara, T. Kambe and K. Oshima, *Phys. Rev. B: Condens. Matter Mater. Phys.*, 2005, **71**, 174424.
- 16 D. V. Konarev, S. S. Khasanov, S. V. Simonov, E. I. Yudanov and R. N. Lyubovskaya, *CrystEngComm*, 2010, **12**, 3542.
- 17 R. Ciancanelli, B. C. Noll, D. L. DuBois and M. Rakowski DuBois, *J. Am. Chem. Soc.*, 2002, **124**, 2984.
- 18 K. Kuwata and D. H. Geske, *J. Am. Chem. Soc.*, 1964, **86**, 2101.
- 19 D. V. Konarev, S. S. Khasanov, E. I. Yudanov and R. N. Lyubovskaya, *Eur. J. Inorg. Chem.*, 2011, 816–820.
- 20 T. Picher, R. Winkler and H. Kuzmany, *Phys. Rev. B: Condens. Matter*, 1994, **49**, 15879.
- 21 N. V. Semkin, N. G. Spitsina, S. Krol and A. Graja, *Chem. Phys. Lett.*, 1996, **256**, 616.

- 22 D. V. Konarev, S. S. Khasanov, G. Saito, A. Otsuka, Y. Yoshida and R. N. Lyubovskaya, *J. Am. Chem. Soc.*, 2003, **125**, 10074.
- 23 T. Ohishi, K. Kashiwabara, J. Fujita, S. Ohba, T. Ishii and Y. Saito, *Bull. Chem. Soc. Jpn.*, 1986, **59**, 385.
- 24 Y. Imamura, T. Mizuta, K. Miyoshi, H. Yorimitsu and K. Oshima, *Chem. Lett.*, 2006, **35**, 260.
- 25 W. W. Brennessel, V. G. Young Jr. and J. E. Ellis, *Angew. Chem., Int. Ed.*, 2002, **41**, 1211.
- 26 D. V. Konarev, S. S. Khasanov, A. Otsuka, Y. Yoshida, R. N. Lyubovskaya and G. Saito, *Chem.–Eur. J.*, 2003, **9**, 3837.
- 27 D. V. Konarev, S. S. Khasanov, A. Otsuka, G. Saito and R. N. Lyubovskaya, *Chem.–Eur. J.*, 2006, **12**, 5225.
- 28 D. V. Konarev, S. S. Khasanov, G. Saito and R. N. Lyubovskaya, *Cryst. Growth Des.*, 2009, **9**, 1170.
- 29 D. V. Konarev, S. S. Khasanov, A. Otsuka, G. Saito and R. N. Lyubovskaya, *Dalton Trans.*, 2009, 6416.
- 30 T. Mori, A. Kobayashi, Y. Sasaki, H. Kobayashi, G. Saito and H. Inokuchi, *Bull. Chem. Soc. Jpn.*, 1984, **57**, 627.
- 31 S. Saito and A. Oshiyama, *Phys. Rev. Lett.*, 1991, **66**, 2637.
- 32 R. W. Lof, M. A. van Veenendaal, B. Koopmans, H. T. Jonkman and G. A. Sawatzky, *Phys. Rev. Lett.*, 1992, **68**, 3924.
- 33 W. I. F. David, R. M. Ibberson, J. C. Matthewman, K. Prassides, T. John, S. Dennis, J. P. Hare, H. W. Kroto, R. Taylor and D. R. M. Walton, *Nature*, 1991, **353**, 147.
- 34 W. H. Green Jr., S. M. Gorum, G. Fitzgerald, P. W. Fowler, A. Ceuleman and B. C. Titeca, *J. Phys. Chem.*, 1996, **100**, 14892.
- 35 G. M. Sheldrick, *SHELX97*, University of Göttingen, Germany, 1997.